


Photoplethysmography Heart Rate Monitoring: State-of-the-Art Design

Etienne Alain Feukeu, University of Cape Town, South Africa

Simon Winberg, University of Cape Town, South Africa

 <https://orcid.org/0000-0001-5809-2372>

ABSTRACT

Research conducted by the World Health Organisation (WHO) in 2018 demonstrated that the worldwide threat of cardiovascular diseases (CVDs) has increased compared to previous years. CVDs are very dangerous: if timely treatment is not performed, these conditions could become irreversible and lead to sudden death. Prescriptive measures include physical exercises and monitoring of the heart rate (HR). Despite the existence of various HR monitoring devices (or HMDs), a major challenge remains their availability, particularly to people in lower-income countries. Unfortunately, it is also this segment of the population that is the most vulnerable to CVDs. Accordingly, this led the authors to propose the design for an easily constructible state-of-the-art HMD that attempts to provide a highly accessible, lower-cost, and long-lasting solution that would be more affordable and accessible to these low-income communities.

KEYWORDS

Differentiator, Integrator, LED, Photoplethysmography, PPG, Sensor

INTRODUCTION

Recently, an investigation conducted around the world by the WHO demonstrated that cardiovascular-related disease has become the number one killer worldwide (World Health Organisation (WHO), 2017). This is very serious consternation for everyone living in this world. In short, Cardio Vascular Disease (CVD) is any disease or condition that affects the structure or the function of the heart. The big problem here is that unlike in the case of other diseases where the cause can be linked to a specific pathology, CVDs causes are various. This is because any element failure in the Cardio Vascular System (CVS) will automatically expose the individual to CVDs. If a preventive measure is not taken to tackle the problem timely, the affected individual may become a victim of sudden death. Including the heart which acts like a pump of the system, many CVDs cases are related to the blood vessel circulatory canals. Just to name, a few of them include the coronary artery diseases, heart attack, arrhythmias, heart failure, heart valve disease, congenital heart disease, heart muscle disease, aorta disease, blood vessel disease (WebMD, 2016). In view to counteract this phenomenon, some general prescriptive and preventive actions include physical activities, healthy nutrition and regular checkups (Association, 2015). The other dilemma is that in most cases, CVD evolves silently and before one could notice that something isn't working well in the body, it is already too late. Since

DOI: 10.4018/IJEHMC.20210501.aa2

This article, published as an Open Access article on January 15th, 2021 in the gold Open Access journal, the International Journal of E-Health and Medical Communications (IJEHMC) (converted to gold Open Access January 15th, 2021), is distributed under the terms of the Creative Commons Attribution License (<http://creativecommons.org/licenses/by/4.0/>) which permits unrestricted use, distribution, and production in any medium, provided the author of the original work and original publication source are properly credited.

CVDs are directly related to the circulatory blood fluid canal, and the canal being a closed circuit, logically, any burst or obstruction in this canal will affect the rate of blood fluid. Since the blood fluid rate is somehow equivalent to the rate at which the heart is pumping the blood into the vessel, the Heart Rate (HR) monitoring becomes a major concern. This is the main motivation driving the development of a multitude of devices available in the market today for HR monitoring. Besides the variety of existing HR monitoring devices, affordability is still a big problem especially in countries of lower-income revenues. Unfortunately, it was also proved that most affected people leaving with CVDs reside in the third world (World Health Organisation (WHO), 2017). Early detection of CVDs is an advantage because some of them can be treated. However, left untreated, they can lead to serious adverse health problems including hypertension, atrial fibrillation, and stroke. This is one further reason which motivated the invention of the Photoplethysmography (PPG) based HR monitoring. Due to its embedded advantages, which include simplicity, lower cost, reliability, non-invasive, mobility and so on, this technology has become the most prominent amongst its peers.

PPG technology is a non-invasive optical technique that measures blood volume changes (Allen, 2007). In this concept, light is shone at the tissue and the backscattered light is then measured by a photodetector. When light travels through the tissue, it is reflected, scattered, and absorbed. In PPG, the photodetector collects the light that is absorbed in tissue and the resulting signal represents the absorption changes due to the variations in blood volume (Allen, 2007). The PPG signals oscillate with the heart cycle period, due to the rhythmical increase and decrease in the tissue blood volume, resulting in a periodically changing transmission of light (Nitzan. M, Babchenko.A, Khanokh.B, Landau.D, 1998). The signal produced by the photodetector is called photoplethysmogram and contains information on the blood light absorption. While the absorbance of some tissues (e.g., bone, muscle) is a constant and can be termed as the DC component of the PPG signal, the absorbance of arterial blood pulsations can be considered as an AC component (Woods. AM, Queen. JS, Lawson. D., 1991). This AC component contains each individual's unique information, although being a very small portion of the whole signal; it can be extracted and amplified to describe the HR activities.

The current work aims to presents a state-of-art practical Heart rate Monitoring Device (HMD) based on PPG technology. The proposed design was developed and presented in such as to serve as a reference design map for everyone with an intermediate biomedical or electronic engineering background to be able to reproduce, modified or redesign the same type of circuit in a reasonable time without difficulty. Step-by-step explanations of each design configuration, component choice and the reason for the choice are well articulated. The design is simple and effective in the sense that both theoretical and practical developmental aspects are integrated together to build a working PPG based HR monitoring device. The main intention is to contribute to the improvement of world health by enabling lower-income revenues and third world countries to be able to take control of their HR monitoring at cheaper costs with the reproduction of the current proposal.

LITERATURE REVIEW

Based on the integrated nature of the proposed HMD, which is made of two physically integrated main parts known as LED/PD coupling pair choice and the circuit (conditioning and signal processing), the literature has been accordingly presented in two sections. The first section presents a review of the LED design considerations and choice for effective PPG signal detection; whereas the second section reviews the previously proposed practical design circuit.

An effective and quality design is achieved through good theoretical and practical analysis (Zio. E, 2009), added to a appropriate component choice to achieve a dependable solution that is affordable to consumer. In the case of HR design, one of the most important steps is the correct choice of the LED and the PD pair. Therefore, to ensure maximum power transfer, high signal sensitivity while minimizing interferences, the LED wavelength selection is primordial.

In terms of heartbeat sensor wavelength selection, a comparison was made by the authors in (Vizbara. V, 2013) between three distinct wavelengths LED of colors blue (465 nm), green (520 nm) and infrared (940 nm). The resulted analysis demonstrated that the green light PPG has the highest Root Mean Square (RMS) and AC/DC values as well as the lowest Artefact to signal Ratio (ASR) values when using on the wrist. This suggests that the green PPG is more suitable for the wrist sensor application as it penetrates deep enough to sense blood pulsations and is less influenced by the DC component of tissues. However, the penetration of the infrared light is the highest, which makes it reflect with more energy than both green and blue light. That is why the infrared light showed the best results in a forehead. In (Anderson. R. R, Parrish. J. A, 1981), the stratum corneum and epidermis provide an optical barrier primarily by absorption of radiation, and to a lesser degree, by optical scattering. In the ultraviolet region less than 300 nm, aromatic amino acids, nucleic acids, urocanic acid, and melanin can be defined as major epidermal absorbers. In the wavelength region 350-1200 nm, melanin is the major absorber of radiation in the epidermis, especially at shorter wavelengths. The dermis may be considered a turbid tissue matrix with which optical scattering is an inverse function of wavelength and largely defines the depth of optical penetration. Using a comparative analysis between the red (880 nm) and green (525 nm) LED, authors in (Maeda. Y, Sekine. M, Tamura. T, 2011) investigated the utility of reflected green light PPG in comparison with reflected infrared PPG and an electrocardiogram (ECG). The results indicated that the difference in wavelength affects the Component Ratio (CR) and that the CR affects the correlation coefficients of the heart rate and pulse rate, especially at skin temperatures above 38°C. These results suggest that reflected green light PPG has an advantage over reflected infrared PPG. In terms of real practical LED wavelength selection for optimal signal sensitivity and detection applicable to PPG, very few works were performed without concise or precise clarification on the component choice made. Electronic Project Focus (Elprocus, 2013-2019) proposed a simple design of HR monitoring. The concept and operating principle based on the PPG technique were explained and a sample diagram was proposed. However, the diagram does not provide any information and explanation on the choice of the used components as well as the component value. Making use of the available off-the-shelf sensor, Electronics Hub (Electronics Hub, 2019) proposed a heartbeat circuit diagram with all components clearly indicated, but again no prescription on wavelength range selection was provided. Just like previously mentioned works, (Stephen Woodward. W, 1997) proposed a design of the HR sensor. The theoretical aspect of the operation was explained but without concise clarification on the diagram, components and operating wavelength of choice made.

In terms of the proposed prototype design circuit, authors (Najmurokhman. A, Rahim. R, Kusnandar. K, Wibowo. B, Kurniawan. D. E. and Sumaryat. Y, 2018) proposed a prototype of a heartbeat meter using the DFR0052 vibration sensor, ATmega 16 microcontroller, and android based smartphone to display heartbeat value via a Bluetooth. A real-time heartbeat calculation is performed to create an alert if any anomaly occurs in the heartbeat. The approach makes use of a vibration sensor placed at a certain position of the body to detect the heartbeat and send the data into the microcontroller. Although the authors claimed to achieve an acceptable result, it is practically difficult to believe since the whole body is in perpetual vibration at all times. Furthermore, no details on component choice and configuration were provided. In (Kao. Y, Chao. P. C and Wey. C, 2019), a new photoplethysmography (PPG) module was designed, optimized, and fabricated to obtain a quality PPG signal for high accuracy bio-sensing. The module has four light-emitting diodes (LEDs) in wavelengths of 530, 660, 850, and 940 nm and a photo-diode (PD). The distances between LEDs and PD were optimized for quality PPG signals via maximizing the ratios of pulsatile (ac) to non-pulsatile (dc) components in PPG waveforms. The optimization was carried based on the established optical model that simulates well optics under the user's skin based on Beer-Lambert law. The study also derived the optimal LED/PD distances that lead to maximal ac/dc ratios of PPGs for different wavelengths. Based on experimental results, an ac/dc ratio of 8.02% was achieved by the proposed PPG module as opposed to 6.74% and 6.90% proposed by two other commercial modules. Based on

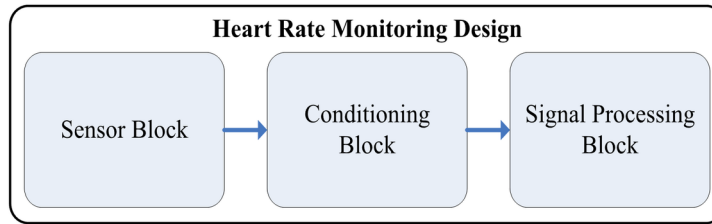
the resulted accuracy, the developed PPG sensor was classified among the bests by the Association for the Advancement of Medical Instrumentation and British Hypertension Society. Well, besides quality result, in terms of practical design implementation, again only a functional block diagram was provided without concise motivation on the component choice and configuration. Authors (Hashem. M. M. A, Shams. R, Kader. M. A and Sayed. M. A, 2010) presented the design and development of a new, economical and integrated HR Measuring (HRM) device. The approach uses optical technology to detect the flow of blood through an index finger based on three conceptual phases which include pulses detection, signal extraction, and pulse amplification. Qualitative and quantitative performance evaluation of the device on real signals shows accuracy in heart rate estimation, even under intense physical activity. Comparative performance evaluation of the HRM device with Electrocardiogram reports and manual pulse measurement results showed that the error rate of the device is negligible. Making use of the commercially available sensors, authors (Rotariu. C, Cristea. C, Arotaritei. D, Bozomitu. R. G and Pasarica. A, 2016) proposed a design and realization of a flexible, scalable and cost-effective device for continuous respiration monitoring and detection of sleep apnea episodes. Respiratory signal measurements are acquired by using a commercially available piezoelectric thoracic belt and processed by the microcontroller in order to compute the respiratory frequency and to detect the sleep apnea episodes. A software application installed on the tablet PC record the information and activates an alert when an apnea episode is detected. Although some circuit diagrams were provided in both (Hashem. M. M. A, Shams. R, Kader. M. A and Sayed. M. A, 2010) and (Rotariu. C, Cristea. C, Arotaritei. D, Bozomitu. R. G and Pasarica. A, 2016), no circuit analysis, component derivation and system configuration were provided. The work of (Yongbo Wan, Xiaodong Sun and Jianchu Yao, 2007) discussed the design of an analog amplification circuit for PPG signals to remove the DC component of the signal. By adding an amplifier bias-adjusting circuit, a high signal-to-noise ratio AC signal was acquired from the raw PPG signal. This hardware improvement resulted in better signal quality and making identification data-processing easier. In (Ghamari. M, Soltanpur. C, Cabrera. S, Romero. R, Martinek. R and Nazeran. H, 2016) a custom-designed wristband-type wireless photoplethysmographic (PPG) device was proposed to collect and analyze the arterial pulse in the wrist. The approach makes use of an optical sensor to monitor arterial pulse, a signal conditioning unit to filter and amplify the analog PPG signal, a microcontroller to digitize the analog PPG signal, and a Bluetooth module to transfer the data to a smart device. A novel model to represent the PPG signal as the summation of two Gaussian functions was also presented. A block diagram was proposed and explained however no specific practical circuit was provided or discussed. A prototype wearable cardiorespiratory monitoring device that could monitor and display the heart rate, respiration rate, peripheral capillary oxygen saturation (SpO₂) and temperature was proposed by (Sasidharan. P, Rajalakshmi. T and Snehalatha. U, 2019). Using a mobile application, captured data are stored and analyzed to predict the HR state and warn the concerned individual beforehand if an abnormality is observed. The proposed design was found to be successful and cost-effective. However, at the exception of the block diagram, no other information was provided in terms of circuit design and implementation.

To this end, to the best of our knowledge, it becomes clear that besides the importance of HR monitoring, a state-of-art design has not yet been very well disclosed. Hence the present work attempts to fill the gap.

DESIGN DEVELOPMENT

Any detector circuit is generally made of three specific blocks namely the sensor, the signal conditioning and the signal processing as depicted in figure 1. The sensor, in this case, is the LED and PD coupling circuit. This is the primary block that transmits and intercepts the infrared signal sensitive to the oxygenated blood flow variation. The signal conditioning block is made of a set of components that participates in transforming the received signal in order to make it easily interpretable by the signal processing block. This conditioning block includes impedance matching, signal translation,

Figure 1. General HR monitoring block diagram



amplification, and filtering. The conditioning block can also be seen as a pre-processing block. The last block is the processing block. It is made to process the signal based on the underlying developed theory such that logical and mathematical analysis, manipulation, interpretation, transformation is possible. The processed signal can also be stored for further analysis.

Sensor Block

This is a combination of the selected LED and the PD coupling block. This is the most important block because if not well designed, it will be difficult to capture the signal of interest. The first most important thing to do before any setup is to make sure that for the chosen components, the frequency responses are matched (LED and PD). This condition is applicable to this work as well as all other design following the same concept and principle. Since several research works have demonstrated that the optimum wavelength highly sensitive to the oxygenated blood is between 660 to 725 Nm, it will be good to choose the LED within this range and thereafter select the corresponding PD of the same response range. In general, based on the proved theory (Wikipedia, 2019) the wavelength can be defined as:

$$\lambda = \frac{h \times C}{E} \quad (1)$$

where E is photon energy, h is the Planck constant defined as a physical constant that is the quantum of electromagnetic action, which relates the energy carried by a photon to its frequency. c is the speed of light in vacuum and λ is the photon's wavelength. As h and c are both constants, photon energy E changes in inverse relation to wavelength λ . The value of Planck constant is $6.62607015 \times 10^{-34}$ (CODATA, 2017) as published by 2018 CODATA.

Considering the LED color identification as being directly related to its average emitting wavelength, to make a corresponding hardware selection based on wavelength response simpler, we employed the approach presented by the authors (Photonics Media, 2019) and (Tutorial, 2019) which involves classifying the signals as per their table 1 and 2.

From these tables, 660 nm (deep red) and 680 nm (Near-IR) are the favourable candidates. However, for a very good response, one must choose a value centred between 660 and 725 nm which is theoretically equal to 692.5 nm; since it is easy to use already made and available frequency range, 680 nm corresponding to the deep red light emission is a preferred good choice for this work. From the selected wavelength of choice, after numerous searches, it was difficult to find the matching frequency response components (LED and PD) from the same vendor. Also because this work is trying to demonstrate how to achieve a good design; it was relevant to choose components from different vendors for this demonstration. The components chosen were the LED680-01AU from Roithner LaserTechnik (RLT) manufacturer (Roithner LaserTechnik, 2012) and the exceptionally stable general-purpose

Table 1. LEDs Wavelengths and Application

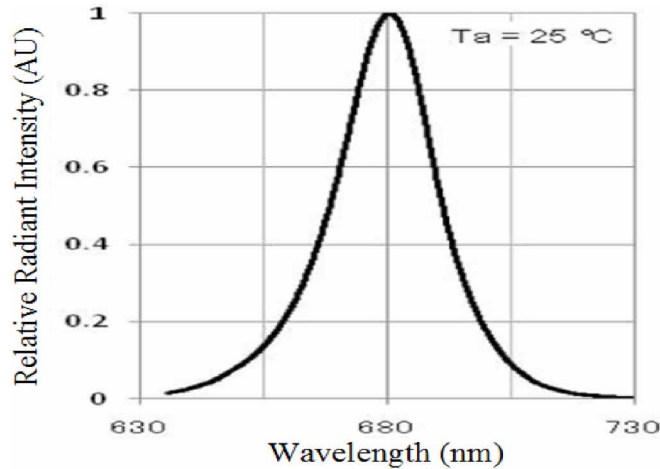
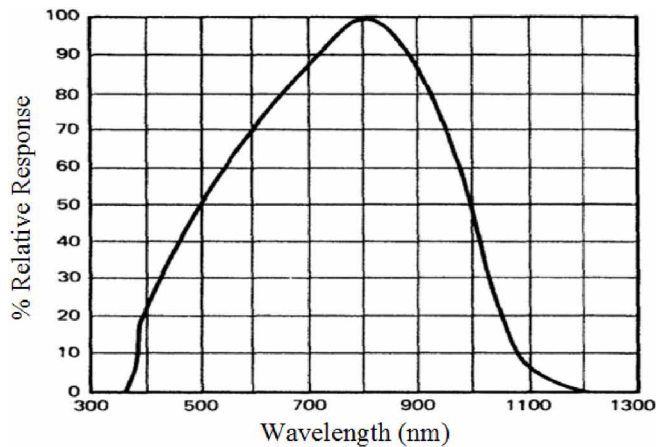


Table 2. Typical LED Characteristics



silicon planar phototransistor FPT 100 from Fairchild manufacturer (FairchildSemiconductor). The frequency response spectrum of the LED and the PD is depicted in figure 2 and figure 3 respectively.

Looking at both figures, it can be observed that the maximum power radiation of the LED will be centred at 680 nm and the PD will be able to perceive at least 80% of the emitted radiation. This is because, in the absence of finding the right PD component with the peak sensitivity at 680 nm, the only closely related one found to the best of our knowledge was the FPT 100 with a peak sensitivity of 800 nm. Since the need was to make use of off-the-shelf available components, FPT 100 was definitely the best choice at the time of this work.

Once the choice of the LED and PD are completed, the next step is to define the Optical Transfer Function (TFo) between the LED and the PD. In general, the transfer function is the ratio of the output over the input value. In this work TFo is the ratio of the received to the emitted radiant power and can be defined as:

Figure 2. RLT LED response curve

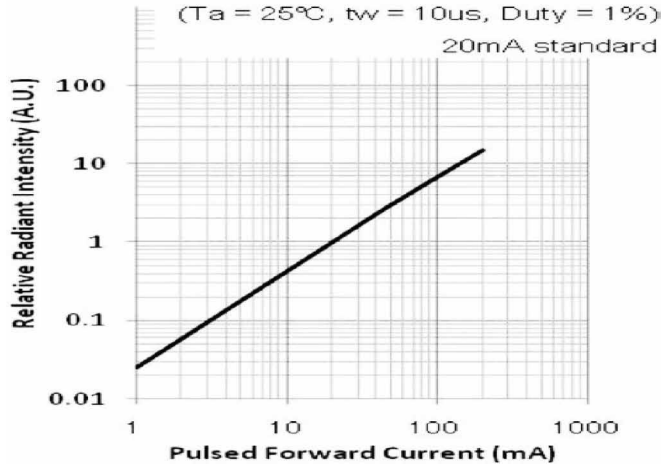
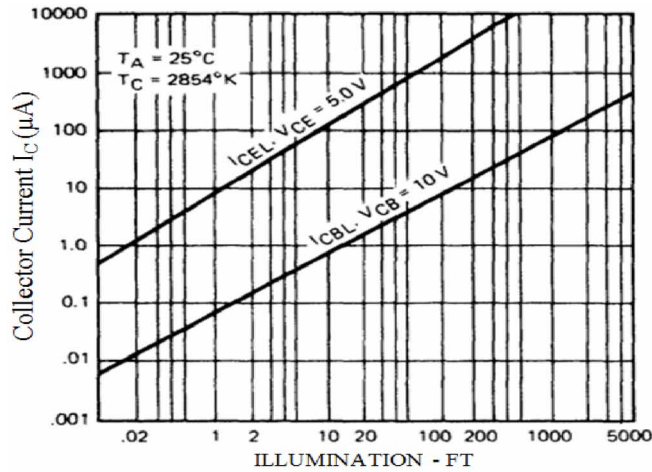


Figure 3. Fairchild FPT100 PD response curve

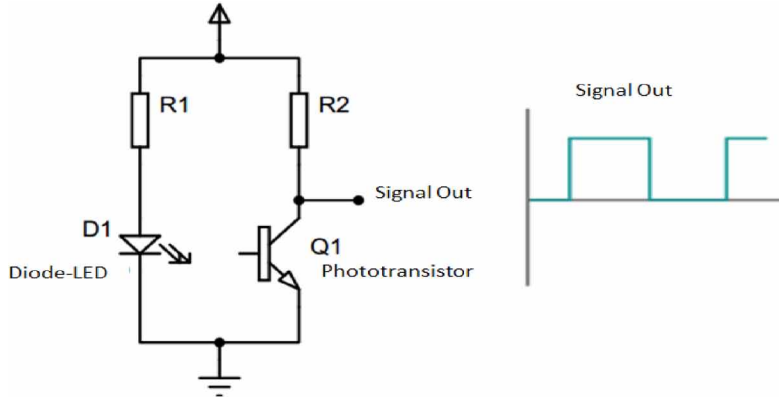


$$TF_o = \frac{\varnothing_r}{\varnothing_e} \quad (2)$$

where \varnothing_r is the received radiant power with \varnothing_e being the emitted radiant power.

It is to note that this TFO takes into account all parameters of the optical link between the LED and the PD. This includes sensor parameters such as resolution, sensitivity, operating range and reflection. It should also be noted that a variation of any abovementioned parameter will directly affect the TFO accordingly. In the case of this work, the term PD was used as a short form to describe the phototransistor because its short abbreviation will be literally confusing at the first look. That is why PD was adopted as its short description. Since the received PD is a transistor and the transmitter been an LED, it makes sense to defined the ratio of the collector current I_c of the phototransistor to the forward current I_F of the LED (I_c/I_F) as a directly and easily measurable optical transfer function.

Figure 4. Radiated luminosity vs. Forward current of the LED



In the case of the optocoupler, the ratio I_c/I_F is generally known as a coupling factor (k). It was demonstrated by (Vishay) that an approximation between TFO and k can be achieved by:

$$K = \frac{I_c}{I_F} = \left[\frac{(S \times B)}{h} \right] \times \frac{\phi_r}{\phi_e} \quad (3)$$

where B is the current amplification and the phototransistor's spectral sensitivity (S) defined as:

$$S = \frac{I_b}{\phi_r} \quad (4)$$

and the proportionality factor between the I_F and ϕ_e (h) is defined as:

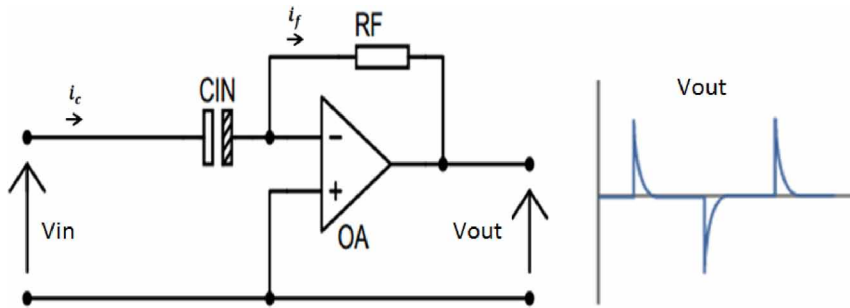
$$h = \frac{I_F}{\phi_e} \quad (5)$$

The response curves contributing to the derivation of the TFO based on both components are presented in figure 4 for the Led and figure 5 for the PD.

A general look at these figures confirms that a very strong and linear relationship exists between the LED light and the produced output current I_c . This is justified by the fact that as the forward current increase, the radiated emitted light power increase from the LED side while from the PD side, as the received illumination intensity increase, the higher the produced output current amplitude. Based on the transmission medium characteristics and the traveling distance between the LED and the PD, the value TFO can then be easily quantified.

The LED and PD coupling circuit, as well as its expected output response, are presented in figure 6. A general look at the figure output demonstrates that the output signal is either ON (logic High when the PD is not conducting in the absence of light) or OFF (logic Low when the PD is conducting as a result of illumination).

Figure 5. Collector current vs. Illumination of the PD



Conditioning Block

This block is essential and acts as an intermediate between the sensor and the processing unit. Also known as the pre-processing block, it is developed and designed as a function of the type of signal delivered by the sensor. In the case of HR, and based on the sensor configuration, the sensor delivers a compound signal component (a mixture of DC and alternative) which is in sync with the oxygenated blood flow movement. In essence, the sensor output is in the form of a variable DC voltage level with only two states (ON or OFF) which can be assimilated to a square wave. In the HR design, because we are interested in HR variation, and based on the mathematical underlying concept, the received sensor signal must logically undergo the first derivation. In the field of electronics, the derivation is achieved with the differentiator circuit. This explains why the first stage of the conditioning circuit is constituted as a differentiator. Since the signal is obtained by differentiation on its first stage, the final stage of the signal will be integrated in order to recover the true useful signal which is the reflection of the HR variation. This concept of integration after derivation in order to obtain the original signal has also been widely and clearly explained and demonstrated in mathematic. A differentiator circuit is needed for many reasons:

- DC blocking which only allows a variable signal to pass through. In general, the capacitor acts as an open circuit if there is no frequency variation, it only conducts if the input signal frequency is not equal to zero. This is justified by the dynamic behaviour of its capacitive reactance as defined in equation 6:

Figure 6. LED and PD coupling circuit

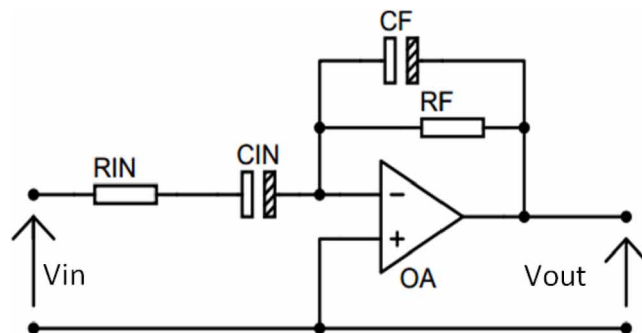
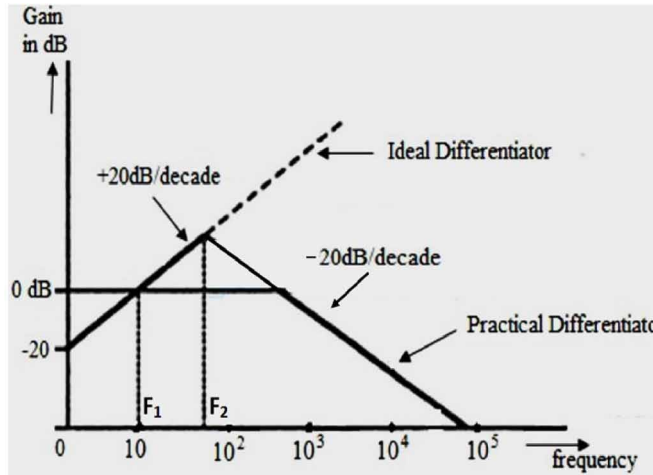


Figure 7. Ideal differentiator circuit



$$X_c = \frac{1}{C \times 2 \times \pi \times f} \quad (6)$$

The analysis of this basic formula proves that as the frequency start increasing, the reactance X_c will behave much more like a normal resistor with value changing from maximum infinite at the frequency of zero Hertz to a minimum zero-ohm when the frequency rises to a certain value based on the capacity of the capacitor.

- Background noise attenuation and discrimination are translated by better signal measurement and precision.
- Peak signal detection because since the differentiation employs a linear technique, the amplitude of the derivative is mostly proportional to the original signal. This process facilitates peak signal detection and signal quantification (Tom. O, 2018).

For illustration purposes, a sample differentiator circuit and its output are presented in figure 7. It is to note that the output as depicted in figure 7 is only obtainable if the differentiator input signal corresponds to the output signal of the figure 6.

Based on the above basic circuit, it will be good to perform some analysis. Based on the fundamental circuit analysis, the negative input of the OA is considered as been virtually grounded. Then if the signal $V(t)$ is applied to the input of the differential amplifier, the current flowing through the capacitor i_c will be equal to i_r .

For recall, the general definition of the current flowing through the capacitor is defined as:

$$i_c = C \frac{dV_c}{dt} \quad (7)$$

then:

$$i_f = \frac{v_F}{R_F} \quad (8)$$

and:

$$v_F = (0 - v_{out}) \Rightarrow v_F = -v_{out} \quad (9)$$

Therefore:

$$i_c = i_f \Rightarrow C \frac{dV_c}{dt} = \frac{-v_{out}}{R_F} \quad (10)$$

$$v_{out}(t) = -R_F \times C \times \frac{dV_c}{dt} \quad (11)$$

For practical implementation, the ideal differentiator as presented in figure 7 suffers from:

- Uncertainty due to the fact that as the input signals frequency increase to a certain level, the capacitive reactance becomes almost zero. Considering the amplification gain formula defined as:

$$A = -\frac{R_F}{R_{IN}} \quad (12)$$

- If the value of R_{IN} become zero, then the amplification gain A will run to infinity. This effect will drive the whole system to Uncertainty. Henceforth, to overcome this problem, a resistor must be connected in series with the input capacitor so that in case the reactance run to zero then input resistance will be limited by the input resistor.
- Instability due to oscillations. The oscillation occurs when the input signal amplitude changes the state from minimum to maximum at the rate faster than the whole system response time. Therefore, due to the feedback effect, instability occurs automatically. To avoid this problem in practice, a small capacitor is inserted in parallel with the feedback resistor.

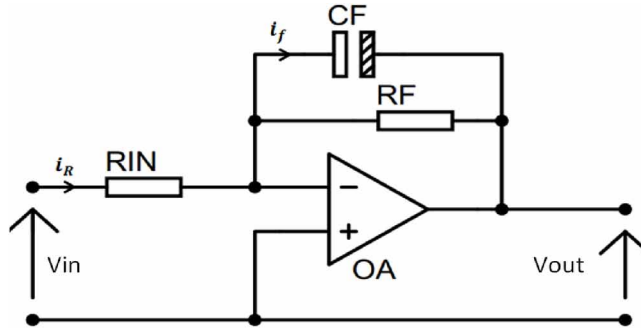
Therefore, the adopted first stage differentiator circuit will be as presented in Figure 8.

The addition of resistor R_1 and capacitor C_f stabilizes the circuit at higher frequencies and also reduces the effect of noise on the circuit.

At this stage, the values of the capacitors are defined based on the cut off frequency of the signal of interest. Since the concern is the signal integration, the cut-off frequency F_2 for the signal will also be the same cut off frequency for the feedback capacitor and it is defined as:

$$F_2 = \frac{1}{2 \times \pi \times R_{IN} \times C_{IN}} \quad (13)$$

Figure 8. Adopted differentiator circuit



where C_{IN} can be derived and C_F also derived just by replacing C_{IN} by C_F in the formula. Thereafter, the signal frequency that can be differentiated must be less than F_2 and greater than F_1 defined as:

$$F_1 = \frac{1}{2 \times \pi \times R_{F \times} C_{IN}} \quad (14)$$

It is to note that this differentiator circuit also acts as a special form of a bandpass filter which starts conducting only from signal frequency F_1 until F_2 .

Based on the defined formula, the frequency response of the differentiator will be in conformance with figure 9 as described in (Electronics Hub, 2019). Having completed the first stage, the last stage will be integrated to recover the HR signal. This is made possible by using the integrator circuit.

This part of the circuit not only will act as an active low pass filter, but it will also sharpen the signal. It does so by integrating the amplitude of the input signal over time to achieve the output. That is why it is sometimes called signal totalizer. In other words, the magnitude of the output signal is determined by the length of time a voltage is present at its input as the current through the feedback loop charges or discharges the capacitor as the required negative feedback occurs through the capacitor (AspenCore, 2019). An integrator circuit is presented in figure 10.

Figure 9. Response curve of the adopted differentiator

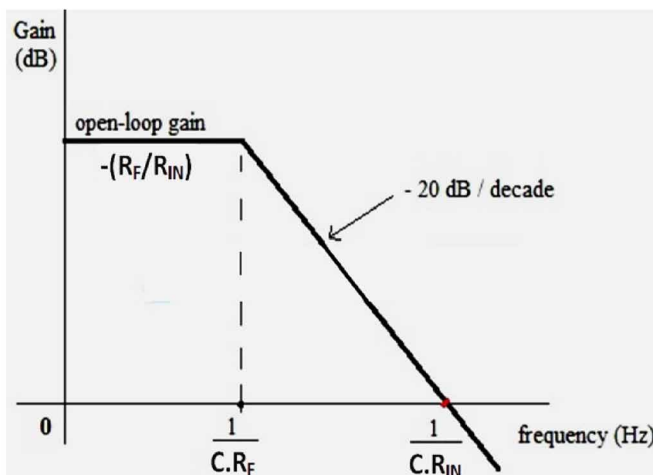
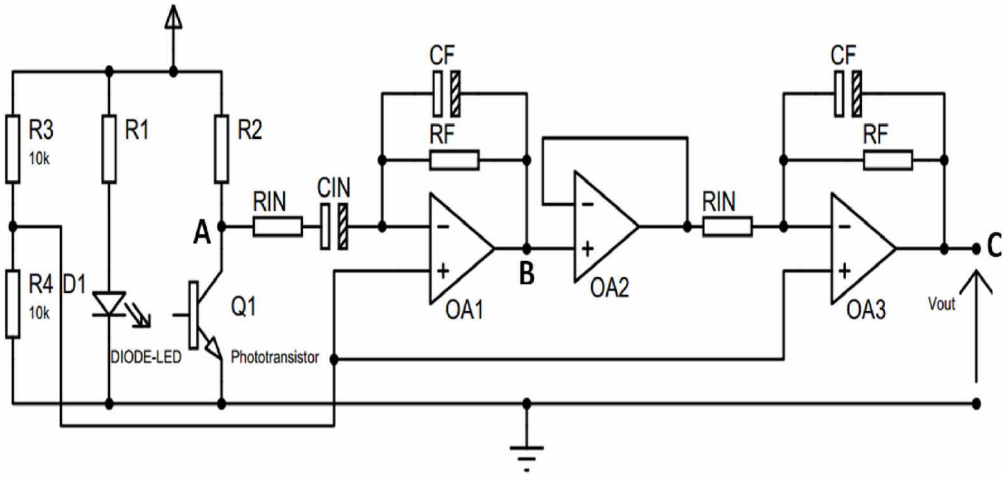


Figure 10. Integrator circuit



Using the same analogy as in the previous figure, in the ideal integrator, the resistor R_f is omitted. However, in practice, R_f helps us achieve a controlled amplification gain when the capacitor reactance is still very high particularly at a lower frequency as defined in equation 12. Based on the virtual ground assumption at the negative input of the OA:

$$i_R = i_f = C \frac{dV_c}{dt} \quad (15)$$

then:

$$V_c = 0 - V_o \Rightarrow V_c = -V_o \quad (16)$$

and:

$$i_R = \frac{V_{in}}{R_{IN}} \quad (17)$$

Therefore:

$$\frac{V_{in}}{R_{IN}} = -C \frac{dV_{out}}{dt} \quad (18)$$

so that:

$$\int \frac{V_{in}}{R_{IN}} dt = -C \int \frac{dV_{out}}{dt} dt \Rightarrow -CV_o = \int \frac{V_{in}}{R_{IN}} dt \quad (19)$$

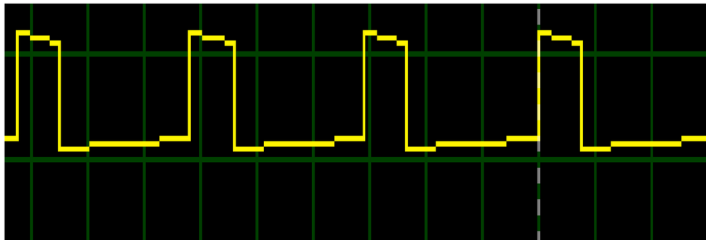
and:

$$V_{out} = -\frac{1}{C \times R_{IN}} \int V_{in} dt \quad (20)$$

This V_{out} expression shows that the output voltage is the inverse time constant of the integrated input voltage and its frequency response curve in conformance with (AspenCore, 2019) is depicted in figure 11.

The response curve of figure 11 clearly demonstrates that the developed integrator is also an active low pass filter with a cut off frequency limited by $1/C.R_F$. Comparable to an active low pass filter, its main advantage is that it provides a relative constant gain between the integration bands comprises below the cut off band.

Figure 11. Integrator response curve



Processing Block

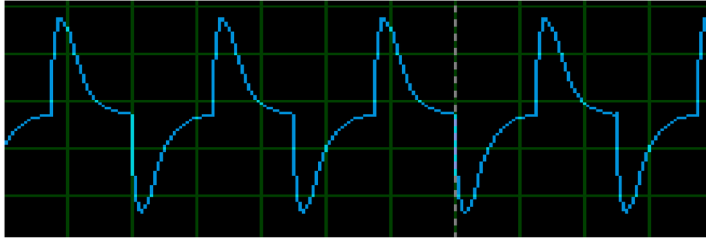
This is where the signal is processed, in the case of HR monitoring; this block is responsible for analysing the received signal and providing a corresponding response. This part has some sort of internal intelligence to analyse and process the received signal. In general, this part is done by a microcontroller or any other processor with some embedded intelligence. Since the focus of this work is on the hardware design, for simplicity, in this work a small program was developed to track, count, and averages the number of pulses per minute for visual display purpose. This block will be represented by a microcontroller.

Final Circuit

In this final circuit, two important remarks can be noted:

- The single supply voltage (generally 4.5 to 6v) battery for a dual voltage OA. This is made possible by connecting the positive supply pin (+ Vs) of the OA to the positive polarity of the battery and connecting the negative supply pin (-Vs) of the OA to the negative polarity or the ground of the battery. This will allow the output voltage to swing from +Vs to zero instead of +Vs to -Vs. Now the problem is that since the input signal will be variable, there will be signal clipping when the negative part of the signal will go through the OA. Therefore, to avoid such problem, the other input of the AO which was made to be connected to the ground is connected to the half voltage level of the supply (that is half of the supply voltage). This arrangement is obtained by the voltage divider components made by resistors R3 and R4. In general, since the working concept of the OA is based on differential amplification of the signal presented at its

Figure 12. Final circuit



two inputs, if one of the input is sitting at the fixed half supply voltage level, then any variable signal applied to the other input with peak to peak output voltage level not greater than 40% of the supply voltage will pass through without attenuation, deformation or deterioration.

- The insertion of the voltage follower or buffer circuit (OA2). The main reason is that based on the appealing inputs/output characteristics of the OA, which present very high input impedance and low output impedance, to avoid the signal drop and ensure maximum signal transfer from the differentiator to the integrator circuit, a voltage follower is needed. Because, mathematically, the low output resistance of the OA1 will be in series with the high input resistance of the OA2. Now just by using ohm law, it can be demonstrated that the maximum voltage of the series combination will be across the very high input resistor of OA2 which in other way guarantees a sufficient condition for the maximum power transfer from OA1 to OA2. It is to note that the voltage follower is a unity gain amplifier and is generally used to drive a heavy load, impedance matching situation or input (source)/output isolation. That is why it was important to be inserted in this design.

TESTING AND VALIDATION

In order to ensure that the proposed design will work accordingly, some routine tests were performed on Proteus design platform software. Since the LED/PD pair was not available on the Proteus platform, a 25% pulse width modulation (PWM) signal of 10 mV amplitude at the frequency of 2 Hz was generated in software and feed in on the input point A of the circuit. This point-A of the circuit corresponds to the output point of the PD. The reason for using this signal is justified by the fact that based on the proposed circuit configuration, the PD will either goes ON or OFF depending on the LED reflected illumination. This ON and OFF state can, therefore, be assimilated to a PWM signal as depicted in figure 13.

Figure 13. Input PWM signal at point A

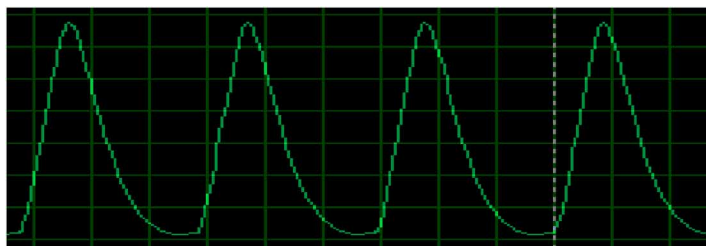
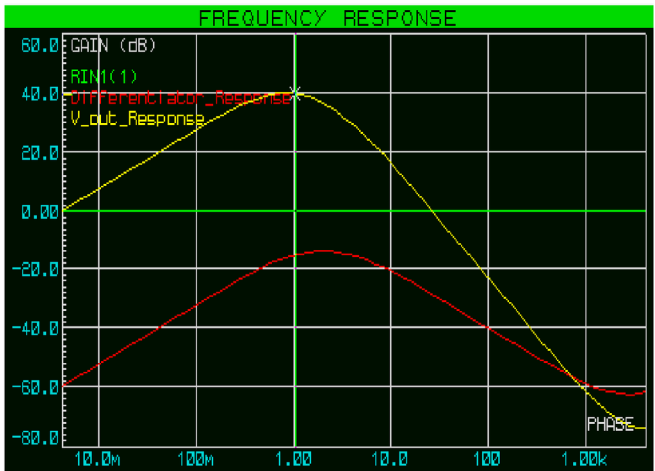


Figure 14. Output signal at point B



The input signal is applied at the input of the differentiator (at point A) and based on the design configuration, it is therefore differentiated and as a result, the output of this first stage (at point B) is converted to the signal depicted in figure 14. Since the OA2 is just a buffer, the same signal of figure 14 is also present at its output which is the input stage of the integrator.

After the integration, the resulted signal which can be assimilated to the PPG signal is presented at the output of the integrator (at point C) and depicted in figure 15.

It is to note that any variation of the pulse width will deform or transform this signal to look very or less closely like that of the true PPG. In general, the amplitude of the recorded PPG signal is critical and can be contaminated by noises from different origin such as Motion artifacts (MA), high-frequency artifacts caused by power source interference, temperature variations, ambient light at the photodetector, poor blood perfusion in the site of monitoring and so on (Luke. A, Shaji. S and Unnikrishna Menon. K. A, 2018). These artifacts corrupt the PPG signal and create confusion between the noise and the true PPG signal. Fortunately, some of these artifacts are cleaned out during

Figure 15. The assimilated PPG signal at point C

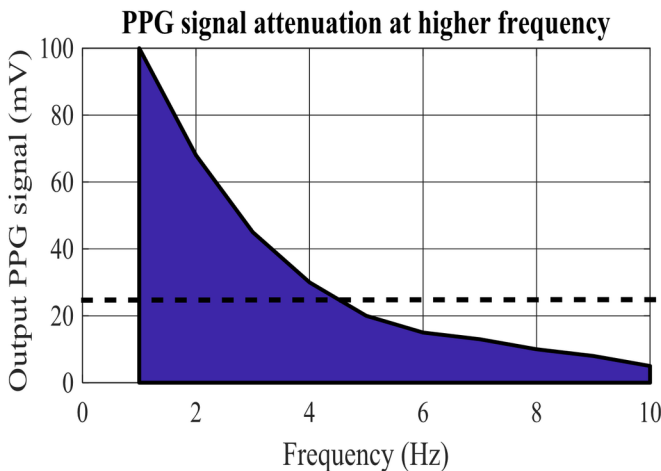
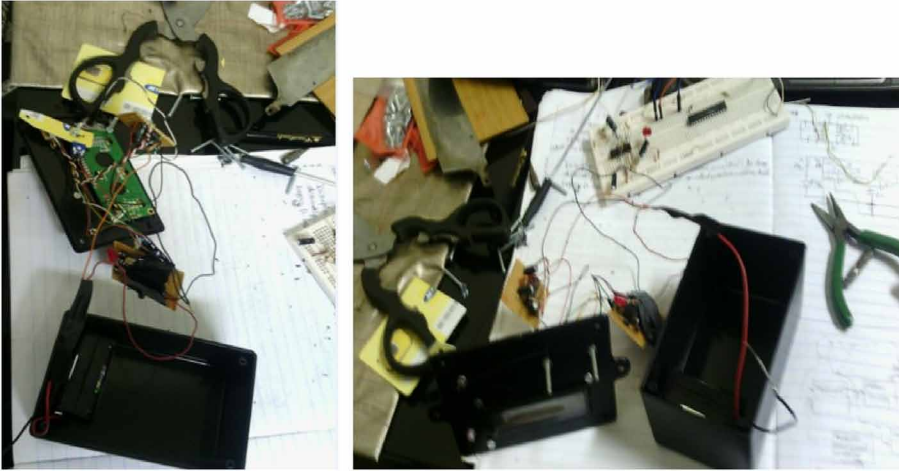


Figure 16. Frequency response curve



the signal processing stage while the first two (MA and high-frequency artifacts) are handled by the hardware design.

Now to make sure that the proposed circuit will be able to reject the motion artifact (MA) and some high frequencies components greater than the PPG signal operating range (greater than 4 Hz), a bode plot frequency response curve was generated and presented in figure 16. Looking at this response, it can be observed that the circuit will only accept frequencies centred around 1 Hz, thereby eliminating some MA problems. The first filter is performed by the differentiator circuit. It can also be observed that the maximum response occurs around 1 Hz and then from about 10 Hz, the output filter attenuates the signal to almost ground level. This action is performed by the integrator circuit. Therefore, the overall response presents us with the PPG HR monitoring device which accepts signal frequency centred around 1 Hz which can be extended up to 4 Hz. The range of 1 to 4 Hz is justified by the fact that in normal circumstances, the HR range between 60 to 160 Beats Per Minute (BPM). Figure 17 also portrays the output signal attenuation graph demonstrating how the signal will get attenuated as the input signal frequency increases. It can be noticed in the same figure how the amplitude gets attenuated to almost 25% at 4 Hz which literally corresponds to 240 BPM. However,

Figure 17. Output PPG Signal attenuation response curve



Figure 18. Assembly phase

LED Wavelength (Color)	LED Applications
410–420 nm (Violet)	Skin therapy
430–470 nm (Blue)	Dental curing instruments
470 nm (Blue)	White LEDs using phosphor
520–530 nm (Green)	Green traffic signal lights
580–590 nm (Amber)	Amber traffic signal lights
630–640 nm (Red)	Red signal lights
660 nm (Deep Red)	Blood oximetry
680 nm (Deep Red)	Blood analysis
800–850 nm (Near-IR)	Night-vision illuminators and beacons for use with night-vision goggles or CCDs
850–940 nm (Near-IR)	Photoelectric controls
940 nm (Near-IR)	Covert illumination CCD-based systems

for frequency lesser than 3 Hz corresponding to a maximum of 180 BPM, the signal amplitude will be greater than 50% which guaranty a good signal strength with high resilience to noises.

Based on the aforementioned development concept, a working PPG HR monitoring device was developed as demonstrated in figures 18 with the final product enclosed in figure 19. This design used an Integrated Circuit (IC) LM348 which is an IC containing 4 OA in the same package. Whenever someone when to check its HR, the device is switched ON and the finger is placed above the LED/ PD pair. Then the PPG signal from the finger is recorded processed and after a couple of seconds, the result is displayed in terms of the number of BPM and as well as in terms of the Inter-Beat Interval (IBI). During the recording period, the signal light is flicking at the tune of the HR.

Figure 19. Working prototype

Typical LED Characteristics			
Semiconductor Material	Wavelength	Colour	V _F @ 20mA
GaAs	850-940nm	Infra-Red	1.2v
GaAsP	630-660nm	Red	1.8v
GaAsP	605-620nm	Amber	2.0v
GaAsP:N	585-595nm	Yellow	2.2v
AlGaP	550-570nm	Green	3.5v
SiC	430-505nm	Blue	3.6v
GaInN	450nm	White	4.0v

CONCLUSION

Taking advantage of the PPG technology (simplicity, mobility, reliability, non-invasiveness, etc), the present work essentially seeks to contribute to the improvement of the world health condition by proposing a state-of-art working prototype HR monitoring device. Preliminary research was conducted to identify the gap in order to justify and motivate the importance of the current proposal. All design steps were well articulated starting from the optical coupling of the sensor block, the signal conditioning requirement from the conditioning block to the expected output from the final design. Since one of the objectives was to enable possible reproduction, modification, or improvement by any other person knowledgeable to the field of electrical, electronic or biomedical engineering, all blocks were designed from scratch to ensure high transparency in all design phases. Thereafter, a final design incorporating all components based on the previously presented design steps was proposed. The proposed state-of-art HR monitoring circuit was then tested and validated in simulation to demonstrate that not only the envisaged objective was achieved, that the output response curve, as well as the whole system frequency response, are all well working within the prescribed boundaries of the PPG signal. The result of this work is indeed a low-cost HR monitoring solution open to the whole world. The economically disadvantaged or low-income countries can take advantage of this proposal to monitor, control and reduce the risks associated with CVDs, thereby improving their local health condition which therefore will have a good positive impact in terms of global life quality.

The particularity of this proposed design is multiple. First, it is unique in the sense that all steps undertaking to achieve the design are easily verifiable to ensure a high degree of confidence. Second, any component choice and configuration steps are well articulated and clarified in order to trigger and serve as a roadmap for any future similar design type. Third, the convergence of the theoretical knowledge with that of the practical skills is integrated to prove the solid existential bond between both. Fourth, the interoperability concept of product integration from different manufacturers using component datasheets is illustrated to broaden the design experiment gained in this work into any other field of interest.

ACKNOWLEDGMENT

This research was supported by the South African Radio Astronomy Observatory, which is a facility of the National Research Foundation, an agency of the Department of Science and Technology.

REFERENCES

- Allen, J. (2007). Photoplethysmography and its application in clinical physiological measurement. *Physiological Measurement*, 28(3), R1–R39. doi:10.1088/0967-3334/28/3/R01 PMID:17322588
- Anderson, R. R., & Parrish, J. A. (1981). The optics of human skin. *The Journal of Investigative Dermatology*, 77(1), 13–19. doi:10.1111/1523-1747.ep12479191 PMID:7252245
- AspenCore. (2019). *The integrator Amplifier*. Retrieved August 28, 2019, from Electronics Tutorial: https://www.electronics-tutorials.ws/opamp/opamp_6.html
- Association, A. H. (2015, July 31). *All About Heart Rate (Pulse)*. Retrieved from <https://www.heart.org/en/health-topics/high-blood-pressure/the-facts-about-high-blood-pressure/all-about-heart-rate-pulse>
- CODATA. (2017, July 1). *Fundamental Physical Constants*. Retrieved September 24, 2019, from CODATA: <https://www.codata.org/committees-and-groups/fundamental-physical-constants>
- Hub, E. (2019). *Heartbeat Sensor using Arduino (Heart Rate Monitor)*. Retrieved July 10, 2019, from Electronics Hub: <https://www.electronicshub.org/heartbeat-sensor-using-arduino-heart-rate-monitor/>
- Elprocus. (2013-2019). *Heartbeat Sensor-Working & Application*. Retrieved July 10, 2019, from Electronic Project Focus: <https://www.elprocus.com/heartbeat-sensor-working-application/>
- FairchildSemiconductor. (n.d.). *General-Purpose Silicon Planar Phototransistor:FPT100/A/B and FPT110/A/B*. Retrieved July 6, 2019, from FairchildSemiconductor: <https://datasheetspdf.com/pdf-file/228463/FairchildSemiconductor/FPT100/1>
- Ghamari, M., Soltanpur, C., Cabrera, S., Romero, R., Martinek, R., & Nazeran, H. (2016). Design and prototyping of a wristband-type wireless photoplethysmographic device for heart rate variability signal analysis. *38th Annual International Conference of the IEEE Engineering in Medicine and Biology Society (EMBC)* (pp. 4967-4970). Orlando, FL: IEEE. doi:10.1109/EMBC.2016.7591842
- Hashem, M. M. A., Shams, R., Kader, M. A., & Sayed, M. A. (2010). Design and development of a heart rate measuring device using fingertip. In *International Conference on Computer and Communication Engineering (ICCCE'10)* (pp. 1-5). Kuala Lumpur: IEEE. doi:10.1109/ICCCE.2010.5556841
- Kao, Y., Chao, P. C., & Wey, C. (2019). Design and Validation of a New PPG Module to Acquire High-Quality Physiological Signals for High-Accuracy Biomedical Sensing. *IEEE Journal of Selected Topics in Quantum Electronics*, 25(1), 1–10. doi:10.1109/JSTQE.2018.2871604
- Luke, A., Shaji, S., & Unnikrishna Menon, K. A. (2018). Motion Artifact Removal and Feature Extraction from PPG Signals Using Efficient Signal Processing Algorithms. In *International Conference on Advances in Computing, Communications and Informatics* (pp. 624-630). Bangalore: ICACCI. doi:10.1109/ICACCI.2018.8554599
- Maeda, Y., Sekine, M., & Tamura, T. (2011). The advantages of wearable green reflected Photoplethysmography. *Journal of Medical Systems*, 829–834. doi:10.1007/s10916-010-9506-z PMID:20703690
- Najmurokhman, A., Rahim, R., Kusnandar, K., Wibowo, B., Kurniawan, D. E., & Sumaryat, Y. (2018). Design and Implementation of A Low Cost Heartbeat Meter using Vibration Sensor, ATmega 16 Microcontroller, and Android Based Smartphone. In *International Conference on Applied Engineering (ICAE)* (pp. 1-5). Batam: IEEE. doi:10.1109/INCAE.2018.8579383
- Nitzan, M., Babchenko, A., Khanokh, B., & Landau, D. (1998). The Variability of The Photoplethysmographic Signal - A Potential Method for The Evaluation of The Autonomic Nervous System. *Physiological Measurement*, 19(1), 93–102. doi:10.1088/0967-3334/19/1/008 PMID:9522390
- Media, P. (2019). *The market place of the industry photonics buyers' guide: Light-Emitting Diodes: A Primer*. Retrieved June 3, 2019, from Photonics Media: <https://www.photonics.com/Article.aspx?AID=36706>
- Roithner LaserTechnic. (2012). *LED680 Series*. Retrieved July 6, 2019, from Roithner LaserTechnic: http://www.roithner-laser.com/datasheets/led_div/led680-series.pdf

- Rotariu, C., Cristea, C., Arotaritei, D., Bozomitu, R. G., & Pasarica, A. (2016). Continuous respiratory monitoring device for detection of sleep apnea episodes. In *22nd International Symposium for Design and Technology in Electronic Packaging (SIITME)* (pp. 106-109). Oradea: IEEE. doi:10.1109/SIITME.2016.7777255
- Sasidharan, P., Rajalakshmi, T., & Snekhalatha, U. (2019). Wearable Cardiorespiratory Monitoring Device for Heart Attack Prediction. In *2019 International Conference on Communication and Signal Processing (ICCSP)* (pp. 54-57). Chennai, India: ICCSP.
- Woodward, S. W. (1997, December 14). *Build your own heart-rate sensor*. Retrieved July 10, 2019, from Electronic Design: <https://www.electronicdesign.com/displays/build-your-own-optical-heart-rate-sensor>
- Tom, O. (2018, July). *A Pragmatic Introduction to Signal Processing, Differentiation*. Retrieved August 27, 2019, from Differentiation: <https://terpconnect.umd.edu/~toh/spectrum/Differentiation.html#Applications>
- Tutorial, E. (2019). *The Light Emitting Diode (LED)*. Retrieved June 3, 2019, from Electronic Tutorial: https://www.electronics-tutorials.ws/diode/diode_8.html
- Vishay. (n.d.). *Application of Optical Reflex Sensors: Document Number 80107 02-02*. Retrieved July 6, 2019, from Vishay: <https://www.vishay.com/docs/80107/80107.pdf>
- Vizbara, V. (2013). Comparison of green, blue and infrared light in wrist and forehead photoplethysmography. *Biomedical Engineering*, 2016, 78–81.
- Web, M. D. (2016, November 2). *Cardiovascular Diseases*. Retrieved from <https://www.webmd.com/heart-disease/guide/diseases-cardiovascular#1>
- Wikipedia. (2019, October 30). *Photon energy*. Retrieved September 20, 2019, from Wikipedia: https://en.wikipedia.org/wiki/Photon_energy
- Woods, AM, Queen, JS, Lawson, D. (1991). Valsalva maneuver in obstetrics: the influence of peripheral circulatory changes on function of the pulse oximeter. *Anesthesia and Analgesia*, 73(6), 765-71.
- World Health Organisation (WHO). (2017). *Cardiovascular diseases (CVDs): Key facts*. Retrieved from <https://www.who.int/news-room/fact-sheets/detail/cardiovascular-diseases-cvds>
- Wan, Sun, & Yao. (2007). *Design of a Photoplethysmographic Sensor for Biometric Identification*. Academic Press.
- Zio, E. (2009). Reliability engineering: Old problems and new challenges. *Reliability Engineering and System Safety*, 94(2), 125-141. doi:10.1016/j.jress200806002

Etienne Alain Feukeu received a Nat Dip in Electronic Communication 2007, a Bachelor Honours (BTech) in Electrical Eng in 2009, a MTech in telecommunication in 2011 with French South African Institute of Technology (FSATI) at Tshwane University of Technology and a MSc in Electronic and Electrical systems with ESIEE of Paris. He completed his PhD in 2016 from Tshwane University of Technology and postdoctoral studies from Vaal University of Technology and UNISA. He has received several research awards from National Research Foundation (NRF) of South Africa. He has published more than 20 papers at reputed international conferences and journals (IEEE and Elsevier) and has been serving as TPC, reviewers and editorial board member at numerous conferences and various reputed ISI Journals. Research Interest: Analysis, Development and Design of Link Adaptation algorithm in WLAN, MIMO systems, Wireless Sensor Network, Telemetry Systems, Vehicular and Dedicated Short Range Communication (DSRC). Signal processing and mathematical modelling of electronic systems, communication network and Biomedical engineering.

Simon L. Winberg completed his B.Sc. (Hons) in computer science at the University of Cape Town, South Africa, in 1999. He received the M.Sc. in Computer Engineering at the University of Tennessee (Knoxville) in 2002. He completed his Ph.D. in Electrical Engineering at the University of Cape Town in 2010. He worked in the embedded systems industry in South Africa and in the United States, during this time he gained experience in development and testing of embedded systems related to factory line inspection equipment, electric power metering and power management systems, health monitoring systems and radar systems. He is currently a senior lecturer in the Department of Electrical Engineering at the University of Cape Town, involved in undergraduate and postgraduate subjects in computer engineering. His research concerns embedded system design, signal processing and machine learning with application towards radar, radio, medical diagnostic equipment, smargrids, and power management systems.